JOURNAL OF SOLID STATE CHEMISTRY 60, 252–257 (1985)

An Outline of the Stucture of $7Bi_2O_3 \cdot 2WO_3$ and Its Solid Solutions

A. WATANABE*

National Institute for Research in Inorganic Materials, 1-1 Namiki, Sakura-mura, Niihari-gun, Ibaraki, 305 Japan

AND N. ISHIZAWA AND M. KATO

Department of Inorganic Materials, Faculty of Engineering, Tokyo Institute of Technology, 12-1 Ōokayama 2-chome, Meguro-ku, Tokyo, 152 Japan

Received March 1, 1985; in revised form May 20, 1985

This paper gives an outline of the structure of a solid solution based on $7Bi_2O_3 \cdot 2WO_3$. The experimental results using X-ray diffraction methods (precession and powder) showed that $7Bi_2O_3 \cdot 2WO_3$ crystallizes in the space group $I4_1/a$ with $a = 12.5143(5)$ Å and $c = 11.2248(6)$ Å. The number of formula weights per unit cell is 40, when the formula is considered to be of the oxygen-deficient fluorite-type $Bi_{0.875}W_{0.125}O_{1.6875}$. The compound has a substructure based on a defect fluorite-type pseudocubic subcell with $a' \simeq 5.6$ Å. The axial relations between the supercell and subcell are $a \simeq \sqrt{5}a'$ and $c \simeq 2a'$. The solid solution was formed over a limited range of WO_3 content between 21.3 mole% and 26.3 mole% at 700°C. The ordering of metal atoms is discussed and an ideal crystal structure is proposed.

Introduction

In the system Bi_2O_3–WO_3, several investigators (*1–8*) have identified an oxygen-deficient fluorite-type phase related to δ-Bi_2O_3, which is a high-temperature polymorph stable between 730 and 825°C (*2, 9–11*). Table I gives, in chronological order, the reported crystal chemical data for the defect fluorite-type phase. There is some disagreement as to the extent of solid solution, although the equilibrium temperatures were not stated explicitly.

In our reexamination of subsolidus equilibrium relations in the system Bi_2O_3–WO_3, a system most recently described by Hoda and Chang (*8*), we found that the X-ray powder diffraction (XRD) pattern for $7Bi_2O_3 \cdot 2WO_3$ (Table I) showed not only several weak lines but also a splitting of some strong lines indexed on a face-centered cubic (fcc) lattice. It therefore seemed likely that the compound has a symmetry lower than cubic. This suggestion induced us to study the crystal structure of $7Bi_2O_3 \cdot 2WO_3$ and the extent of solid solution. The results show that the true symmetry is tetragonal, $I4_1/a$, and that limited solid solution is formed.

Experimental Procedure

Polycrystalline specimens of composi-

* To whom correspondence should be addressed.

0022-4596/85 $3.00

TABLE I

SUMMARY OF PREVIOUS WORK ON THE OXYGEN-DEFICIENT FLUORITE-TYPE PHASES IN THE SYSTEM Bi_2O_3–WO_3

Source[a]	Composition: WO_3 content (mole%)	Formula	Lattice constant (Å)	Solid solubility: WO_3 content (mole%)
Sillén and Lundborg (*1*)	25.3		5.573	0
	28.6		5.536	0
Gattow and Schröder (*2*)	33.33	$2Bi_2O_3 \cdot WO_3$	5.589	0
Smolyaninov and Belyaev (*3*)	25.0	$3Bi_2O_3 \cdot WO_3$	—	Not determined
Gal'perin *et al.* (*4*)	33.33	$2Bi_2O_3 \cdot WO_3$	5.591	16.7–33.33
Speranskaya (*5*)	25.0	$3Bi_2O_3 \cdot WO_3$	—	16.0–33.4
Takahashi and Iwahara (*6*, *7*)	25.0	$3Bi_2O_3 \cdot WO_3$	5.604	22–27
Hoda and Chang (*8*)	22.22	$7Bi_2O_3 \cdot 2WO_3$	5.61	20.3–23.6[b]

[a] Refs. *1–8*.

[b] Read off the figure reported by Hoda and Chang (*8*) at 700°C.

tion $Bi_{2-2x}W_xO_3$ (where $x = 0.18$–0.29) as well as $7Bi_2O_3 \cdot 2WO_3$ ($x = 0.222$) were prepared by solid-state techniques. The starting materials were 99.9% pure Bi_2O_3 from Iwaki Chemicals, Ltd. and WO_3 from New Japan Metallic Chemistry, Ltd. The desired proportions were weighed and thoroughly mixed in an agate mortar under ethanol. After drying, the mixtures were heated in a covered platinum crucible at 800°C in air for 20 hr. Conventional XRD patterns (diffractometer) using Ni-filtered Cu$K\alpha$ radiation showed that the reaction was complete. To check the solid-solution region, all the specimens were equilibrated at 700°C for 20 hr and then cooled rapidly in air to room temperature.

Single crystals were grown in the following way. The prepared powder with composition $7Bi_2O_3 \cdot 2WO_3$ was packed into a covered platinum crucible. The crucible was heated at a rate of 100°C hr^{-1} to 1050°C and then cooled at a rate of 4°C hr^{-1} through 400°C; at this point the power was turned off. The resulting crystals, which were transparent and homogeneously brownish-yellow, were checked by optical microscopy and the XRD method.

Single crystals of $7Bi_2O_3 \cdot 2WO_3$ were studied by the precession method to obtain preliminary lattice parameters as well as the space group symmetry. A least-squares computer program (*12*) was used to refine the lattice parameters. The solid-solution limits were determined by means of a parametric method (*13*) based on the XRD patterns.

Results and Discussion

Examination of the single crystals with the polarizing microscope showed that they do not have cubic symmetry, and XRD patterns from pulverized single crystals strongly resembled the patterns obtained from polycrystalline specimens of composition $7Bi_2O_3 \cdot 2WO_3$.

Inasmuch as a series of precession photographs, one of which is shown in Fig. 1, displayed Friedel symmetry $4/m$, the true symmetry was tetragonal, and the approximate lattice parameters were $a = 12.50$ and $c = 11.21$ Å. The only reflections present were hkl: $h + k + l = 2n$, $hk0$: $h = 2n$ and $k = 2n$, hhl: $l = 2n$, and $00l$: $l = 4n$, which uniquely determine the pace group as $I4_1/a$ (No. 88) (*14*). Furthermore, the photographs indicated that the structure is based on a subcell, which is a psuedo-fcc cell of dimensions about 5.6 Å. That is, the tetrag-

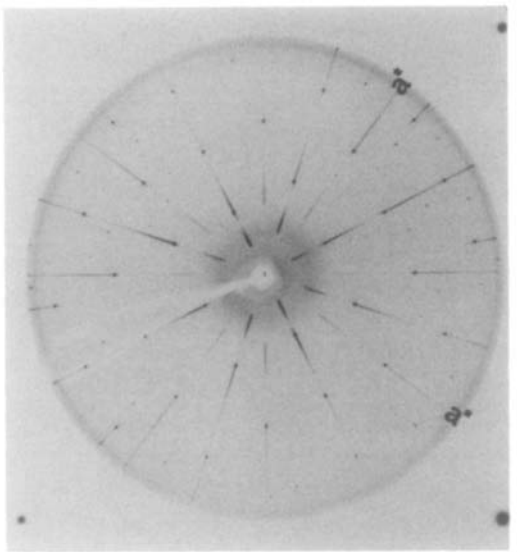

FIG. 1. Zero-level photograph of $7Bi_2O_3 \cdot 2WO_3$ with [001] as the precessing axis using Zr-filtered Mo$K\alpha$ radiation.

onal structure has a substructure similar to the defect-fluorite type listed in Table I, implying the existence of atomic ordering. On the basis of these results, Fig. 2 represents the topotactic relations between the tetragonal cell (a, c) and the pseudo-fcc subcell (a'), namely, $a \simeq \sqrt{5}a'$ and $c \simeq 2a'$. The indices h', k', l' of the subcell are related to the indices h, k, l of the tetragonal cell by the transformation $210/\bar{1}20/002$. The tetragonal cell is 10 times the size of the subcell.

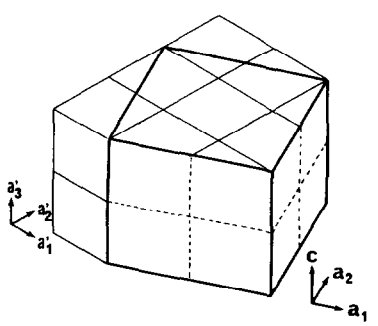

FIG. 2. Schematic representation of the relations of the unit-cell axes. Heavy solid lines show the tetragonal cell (a, c) and weak solid lines outline the pseudo-fcc subcells (a').

Figure 3 shows the variations of the lattice parameters and cell volume with composition. The solid solution $Bi_{2-2x}W_xO_3$ based on this tetragonal structure is formed over a limited range of x between 0.213 and 0.263 at 700°C. Among the compounds tabulated in Table I, $3Bi_2O_3 \cdot WO_3$ ($x = 0.25$), $7Bi_2O_3 \cdot 2WO_3$ ($x = 0.222$), and another ($x = 0.253$) belong to this limited solid solution series. Although the plotted results violate Vegard's law, deviations of this type are found in "defect substitutional solid solutions" (*13, 15*). In fact, since the structure of this solid solution consists of oxygen-deficient fluorite-type subcells, it is reasonable to assume that anomalies in the curves in Fig. 3 are due to vacancies in the partial lattice of oxygen. Also, the oxygen-deficient structure is supported by evidence from the excellent oxide-ion conduction in the $Bi_{2-2x}W_xO_3$ series with $x = 0.22$ to 0.27 (*6, 7*).

The precise lattice parameters of the tetragonal cell for this solid solution were de-

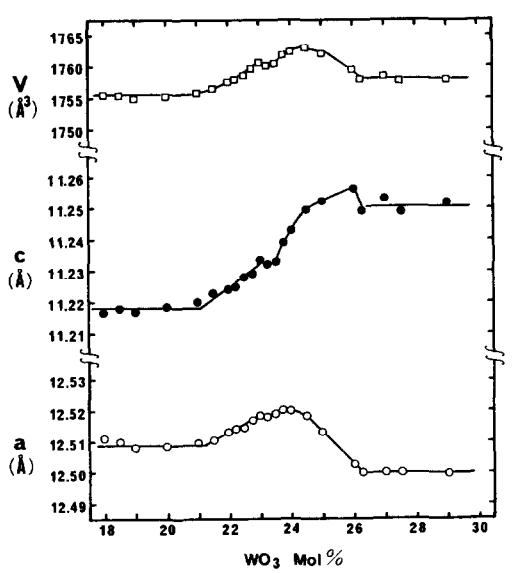

FIG. 3. Variation of lattice parameters and cell volumes at 700°C of solid solutions having the $7Bi_2O_3 \cdot 2WO_3$ structure.

termined by the least-squares method using the foregoing preliminary lattice parameters, examples being $a = 12.5143(5)$ Å, $c = 11.2248(6)$ Å for $7Bi_2O_3 \cdot 2WO_3$, and $a = 12.5132(3)$ Å, $c = 11.2525(3)$ Å for $3Bi_2O_3 \cdot WO_3$. Table II gives the observed and calculated d values and intensities of XRD lines for $7Bi_2O_3 \cdot 2WO_3$ along with the corresponding Miller indices of the pseudo-fcc subcell. Since the intensities of the superstructure reflections are much weaker than those of the fundamental reflections based on the pseudo-fcc lattice, and since the splitting of the XRD lines of the fundamental reflections is quite small, these tetragonal solid solutions might well be erroneously identified as defect-fluorite-type cubic phases.

According to Speranskaya (*5*), $3Bi_2O_3 \cdot WO_3$ has a measured density of 8.64 g $\cdot$ cm^{-3}. Moreover, the general formula of this solid solution $Bi_{2-2x}W_xO_3$ can be represented as an oxygen-deficient fluorite-type formula $(Bi,W)O_{2-x}$. Using these facts, a calculation shows that the tetragonal unit cell of the solid solution contains 40 formula units of $(Bi,W)O_{2-x}$, i.e., $Z = 40$. This value can be also obtained from the cell volume relations shown in Fig. 2, since the fluorite-type unit cell contains 4 formula units of AX_2 and the volume of supercell is 10 times that of the subcell. Consequently, $7Bi_2O_3 \cdot 2WO_3$ can be represented as $(Bi_{0.875}W_{0.125})O_{1.6875}$ and the unit cell contains 35 bismuth atoms, 5 tungsten atoms, and 67.5 oxygen atoms (i.e., about 15.6% of oxygen sites are empty).

At this point, we may infer from the crystallographic results obtained above an outline of "ideal" crystal structure for the solid solutions. As a matter of convenience, we shall take the structure with composition $7Bi_2O_3 \cdot 2WO_3$ as the representative of whole solid solution series. Space group $I4_1/a$ allows the following possible atomic arrangements. Four tungsten atoms can occupy either of the two special positions 4*a* or 4*b*, where these two positions are simply alternative choices for the origin of the unit cell. We shall arbitrarily assign the 4 tung-

TABLE II

X-RAY POWDER DIFFRACTION DATA FOR $7Bi_2O_3 \cdot 2WO_3$

$h\ k\ l$	d_{calc} (Å)	d_{obs} (Å)	I_{obs}	I_{calc}	$h'\ k'\ l'$[a]
1 0 1	8.356	8.373	1	0.06	
2 0 0	6.257	6.266	1	0.08	
2 1 1	5.009	5.013	1	0.04	
2 0 2	4.178	4.180	1	0.00	
1 0 3	3.585	3.587	3	0.01	
3 1 2	3.2342	3.2342	100	100.00	1 1 1
2 1 3	3.1105	3.1093	1	0.01	
0 0 4	2.8062	2.8062	26	12.91	0 0 2
4 2 0	2.7983	2.7986	26	25.80	2 0 0, 0 2 0
3 2 3	2.5446	2.5445	1	0.01	
5 1 2	2.2486	2.2483	1	0.02	
4 4 0	2.2122	2.2087	1	0.01	
4 0 4	2.0890	2.0826	1	0.01	
2 1 5	2.0836			0.01	
4 2 4	1.9815	1.9802	23	33.85	2 0 2, 0 2 2
6 2 0	1.9787			16.91	2 2 0
3 2 5	1.8850	1.8846	<1[b]	0.01	
4 1 5	1.8049	1.8040	1	0.01	
3 1 6	1.6913	1.6917	10	15.04	1 1 3
5 5 2	1.6878	1.6879	19	15.01	1 3 1
7 1 2				15.01	3 1 1
6 2 4	1.6171	1.6172	7	11.46	2 2 2
1 0 7	1.5905	1.5904	<1	0.00	
7 3 2	1.5770	1.5768	<1	0.01	
2 1 7	1.5415	1.5413	<1	0.01	
8 2 0	1.5176	1.5169	1	0.01	
6 1 5	1.5168			0.01	
6 4 4	1.4760	1.4742	<1	0.01	
3 2 7	1.4557	1.4556	<1	0.01	
7 3 4	1.4180	1.4179	<1	0.00	
4 1 7	1.4178			0.01	
0 0 8	1.4031	1.4031	<1	2.70	0 0 4
8 4 0	1.3991	1.3991	2	5.37	4 0 0, 0 4 0
5 2 7	1.3198	1.3202	<1	0.00	
7 1 6	1.2857	1.2858	4	6.45	3 1 3
5 5 6				6.45	1 3 3
9 3 2	1.2841	1.2839	4	6.44	3 3 1
7 4 5	1.2767	1.2769	<1	0.00	
6 1 7	1.2648	1.2652	<1	0.00	
4 2 8	1.2543	1.2540	2	5.17	2 0 4, 0 2 4
8 4 4	1.2521	1.2517	4	5.16	4 0 2, 0 4 2
10 0 0	1.2514			2.58	4 2 0
8 6 0				2.58	2 4 0
2 1 9	1.2173	1.2174	<1	0.00	
3 2 9	1.1737	1.1740	<1	0.00	
6 2 8	1.1445	1.1443	1	4.91	2 2 4
10 0 4	1.1429	1.1429	4	4.90	4 2 2
8 6 4				4.90	2 4 2
3 1 10	1.0799	1.0800	1	3.83	1 1 5
9 3 6	1.0781	1.0780	2	3.82	3 3 3
9 7 2	1.0772	1.0772	3	3.82	1 5 1
11 3 2				3.82	5 1 1

[a] Miller indices for the pseudo-fcc subcell.

[b] Observed relative intensity weaker than 1.

sten atoms to 4*a*. Another tungsten atom and 3 bismuth atoms can statistically occupy the positions 4*b*. The other 32 bismuth atoms can fully occupy two sets of the general position 16*f*. Likewise, all the oxygen atoms are split into five sets and can occupy the positions 16*f* statistically with each position having an average occupancy of 67.5/80 or 84.4%. The positional parameters thus deduced are tabulated in Table III. The calculated intensities juxtaposed in Table II are based on these positional parameters. A schematic of the structure is depicted in Fig. 4; for a clearer understanding of the structure, all oxygen atoms are omitted and the length of the *c* axis is deliberately exaggerated. It is clear from the oxygen-deficient fluorite-type subcell that each metal atom is statistically surrounded by eight equidistant oxygen sites (site occupancy 84.4%), which are arranged at the corners of a cube. Since reasonable agreement between observed and calculated XRD intensities (Table II) was obtained, the actual structure is probably not far from this "ideal" one. Thus, it is probable that the ordering of metal atoms gives rise to the tetragonal superstructure in this solid solution series. Strictly speaking, however, there is a doubt whether each tungsten atom is surrounded by eight oxygen atoms, because the ionic radius ratio, $r(W^{6+})/r(O^{2-})$, is too small for the eight-coordination (cube). Accordingly, a single crystal X-ray diffraction analysis or a neutron diffraction analysis is needed to determine the "actual" crystal structure.

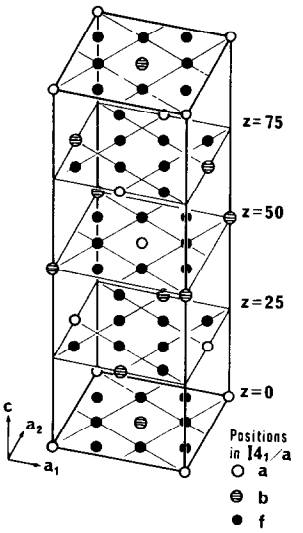

FIG. 4. A perspective view of the unit cell of the idealized tetragonal structure. For clarity, all oxygens are omitted and the length of the *c* axis is exaggerated. Each metal atom (Bi or W) occupies one of two special positions 4*a* and 4*b* or one general position 16*f* in space group $I4_1/a$. The weak solid lines outline the pseudo-fcc subcells.

TABLE III

PROPOSED ATOMIC COORDINATES FOR $7Bi_2O_3 \cdot 2WO_3$ IN THE SPACE GROUP $I4_1/a$[a]

Atom		*x*	*y*	*z*
W	4*a*	0	0	0
		0	0.5	0.25
		0.5	0.5	0.5
		0.5	0	0.75
M[b]	4*b*	0	0	0.5
		0	0.5	0.75
		0.5	0.5	0
		0.5	0	0.25
Bi (1)	16*f*	0.3	0.1	0
Bi (2)	16*f*	0.2	0.4	0
O (1)[c]	16*f*	0.15	0.05	0.125
O (2)	16*f*	0.05	0.35	0.125
O (3)	16*f*	0.25	0.25	0.125
O (4)	16*f*	0.45	0.15	0.125
O (5)	16*f*	0.65	0.05	0.125

[a] $Z = 40$ when the formula unit is the defect-fluorite type $(Bi,W)O_{2-x}$, i.e., $Bi_{0.875}W_{0.125}O_{1.6875}$.

[b] $M = 0.25W + 0.75Bi$.

[c] For all oxygens, site occupancy is 84.4%.

Using the proposed structure for $7Bi_2O_3 \cdot 2WO_3$, we can examine the relationship between solubility limits and structure. That is, from Fig. 3, the solid solution phase $Bi_{2-2x}W_xO_3$ is seen to occur over a limited range of x between 0.213 and 0.263 at 700°C. The unit cell with the lower-limit composition contains 4.76 tungsten atoms. On the other hand, the unit cell accommo-

dates 6.04 tungsten atoms at the upper solubility limit. Considering that the special positions 4*a* are preferentially occupied by four tungsten atoms, the lower-limit value ($x = 0.213$) is reasonable. By contrast, the composition with $x = 0.182$, for which the unit cell contains exactly four tungsten atoms, does not allow the present tetragonal structure; that is, to stabilize this structure, tungsten atoms must partially occupy the special positions 4*b* above a minimum occupancy of 0.76/4 or 19% at 700°C. As for the upper limit, the special positions 4*b* are able to accommodate a maximum of about 2 tungsten atoms, each site being statistically half bismuth and half tungsten. Outside the compositional range of the solid solution, additional phases appear, namely, $7Bi_2O_3 \cdot WO_3$ (*8*) below the lower limit and $Bi_2O_3 \cdot WO_3$ (*16, 17*) above the upper limit.

Speranskaya (*5*) reported that $3Bi_2O_3 \cdot WO_3$ exhibited a reversible phase transition at 900°C. However, Hoda and Chang (*8*) indicated in their phase diagram that the fcc solid solution based on $7Bi_2O_3 \cdot 2WO_3$ did not undergo any solid-state transition but melted incongruently near 900°C as part of a peritectic-type equilibrium. (The peritectic reaction occurred at 965°C.) Our DTA studies showed that this solid solution underwent a solid-state transition at about 900°C as reported by Speranskaya (*5*). This is probably an order–disorder transformation, which seems to result in a high-temperature disordered phase with a true fcc structure. The details of this transition are now under investigation.

References

1. L. G. Sillén and K. Lundborg, *Ark. Kemi, Mineral. Geol. A* **17**(21), 1 (1943).
2. G. Gattow and H. Schröder, *Z. Anorg. Allg. Chem.* **318,** 176 (1962).
3. N. P. Smolyaninov and I. N. Belyaev, *Russ. J. Inorg. Chem.* **7,** 1345 (1962).
4. E. L. Gal'perin, L. Ya. Erman, I. K. Kolchin, M. A. Belova, and K. S. Chernyshev, *Russ. J. Inorg. Chem.* **11,** 1137 (1966).
5. E. I. Speranskaya, *Inorg. Mater. (USSR)* **6,** 127 (1970).
6. T. Takahashi and H. Iwahara, *J. Appl. Electrochem.* **3,** 65 (1973).
7. T. Takahashi and H. Iwahara, *Mater. Res. Bull.* **13,** 1447 (1978).
8. S. N. Hoda and L. L. Y. Chang, *J. Amer. Ceram. Soc.* **57,** 323 (1974).
9. G. Gattow and D. Schütze, *Naturwissenschaften* **50,** 546 (1963).
10. E. M. Levin and R. S. Roth, *J. Res. Nat. Bur. Stand. A* **68,** 189 (1964).
11. H. A. Harwig and A. G. Gerards, *Thermochim. Acta* **28,** 121 (1979).
12. D. E. Appleman and H. T. Evans, Jr., National Technical Information Service PB–216, 188 (1973).
13. B. D. Cullity, "Elements of X-Ray Diffraction," 3rd Printing, pp. 353–358, Addison–Wesley, Reading, Mass. (1967).
14. N. F. M. Henry and K. Lonsdale (Eds.), "International Tables for X-Ray Crystallography," Vol. I, 3rd Ed., Kynoch Press, Birmingham (1967).
15. R. K. Datta and J. P. Meehan, *Z. Anorg. Allg. Chem.* **383,** 328 (1971).
16. R. W. Wolfe, R. E. Newnham, and M. I. Kay, *Solid State Commun.* **7,** 1797 (1969).
17. A. Watanabe, *Mater. Res. Bull.* **19,** 877 (1984).